Horizontal diffusion in the atmosphere as determined by geostrophic trajectories

By C. S. DURST,* A. F. CROSSLEY† AND N. E. DAVIS†
* 7 Alton Road, London, S.W. 15
† Meteorological Office, Air Ministry, London, W.C. 2

(Received 24 April 1958 and in revised form 7 March 1959)

If a series of air trajectories is drawn from a fixed point at a certain height above the earth's surface, the end-points of the superimposed trajectories, after each has been followed for a time t, will have a standard vector deviation S. The purpose of this paper is to discuss the form of S. One expression is obtained by relating S empirically to the magnitude of the mean vector position $[\mathbf{x}]$ of the ends of the trajectories, so that

$$S = CL\,|[\mathbf{x}/L]|^{a},$$

where L is a certain length and C and a are dimensionless constants; a is found to be about 0·870 and C is nearly proportional to $\sqrt{T}$, where T is the total period over which the series of trajectories is initiated.

A more satisfying expression for S connects it with the variability of the wind during the period of initiation of the trajectories, i.e. with the standard vector deviation of wind (σ) which is itself dependent on T. The relationship involves the Lagrangian correlation coefficient $r(t)$ of wind with time along the trajectories. It is found that the variation of S with time t agrees well with that deduced from the exponential formula $r(t) = e^{-\alpha t}$. Moreover, α, the reciprocal of the characteristic time of the 'eddies', is identified with σ^2/K where K is the coefficient of eddy viscosity for lateral mixing.

Introduction

If a trajectory of a particle of the free air is drawn from a point it will follow a meandering path; if at subsequent times a second, third and successive trajectories are initiated from the same point at equal time intervals, their paths will form a plume flowing out in the direction of the general wind stream, as shown in figures 1a and 1b. These plumes are not of exactly the same type as, for example, the plume of smoke from a chimney emitting a continuous source of pollution but are more closely paralleled by the pattern on the ground of the pollution deposited from such a chimney. The analogy is not exact in the case of geostrophic trajectories, because in a smoke plume the individual particles are free to move vertically as well as horizontally, whereas a geostrophic trajectory is the quasi-horizontal path of a point element.

To discuss these plumes of trajectories we should follow the true paths of selected elements of air, but since it is not in general possible to do so on the scale of synoptic charts, there have been substituted instead 'geostrophic

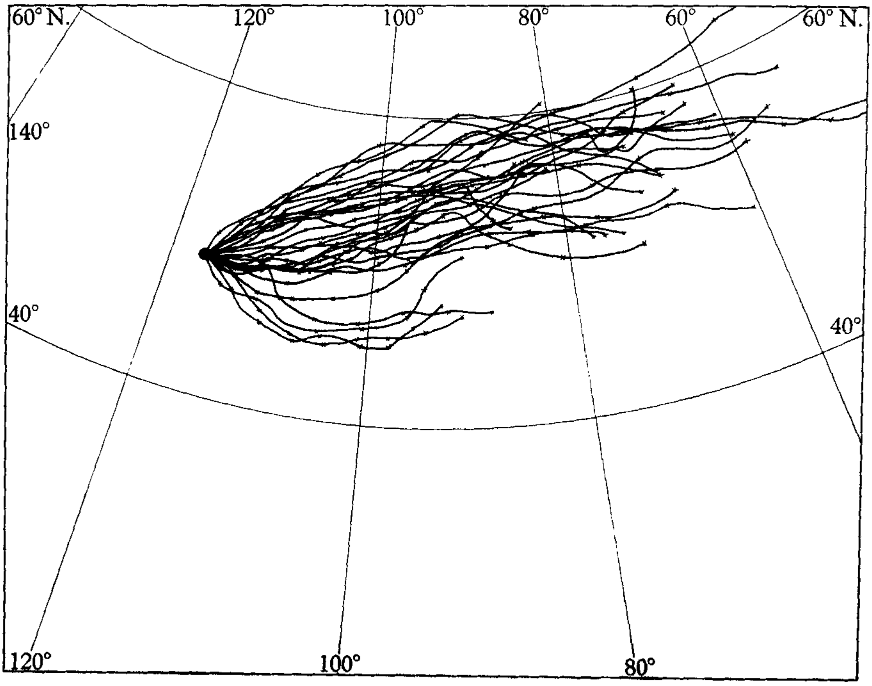

FIGURE 1*a*. Trajectories initiated twice a day and pursued for 4 days during 1–15 Aug. 1947 at 700 mb.

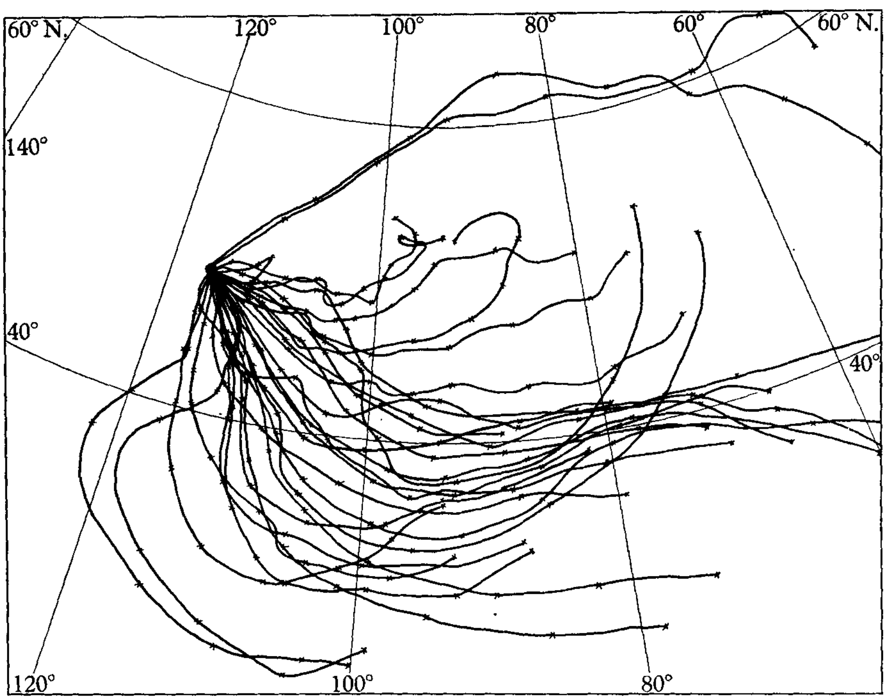

FIGURE 1*b*. Trajectories initiated twice a day and pursued for 4 days during 1–15 Nov. 1947 at 700 mb.

trajectories'. These are formed, according to common practice, by measuring the geostrophic wind near the point of origin on a synoptic or pressure contour chart, plotting the position which the air at that point will have reached after half the time interval to the next chart, measuring the geostrophic wind on the next chart, at the position at which the air will probably have arrived at the time of that (second) chart, drawing the probable track of the air up to the mid-time between the second and third charts and so on. Although individual geostrophic trajectories will no doubt vary at times considerably from the trajectories traced out by the real winds, it is believed that the standard deviation of the end-points of the geostrophic trajectories is not very different from that of the

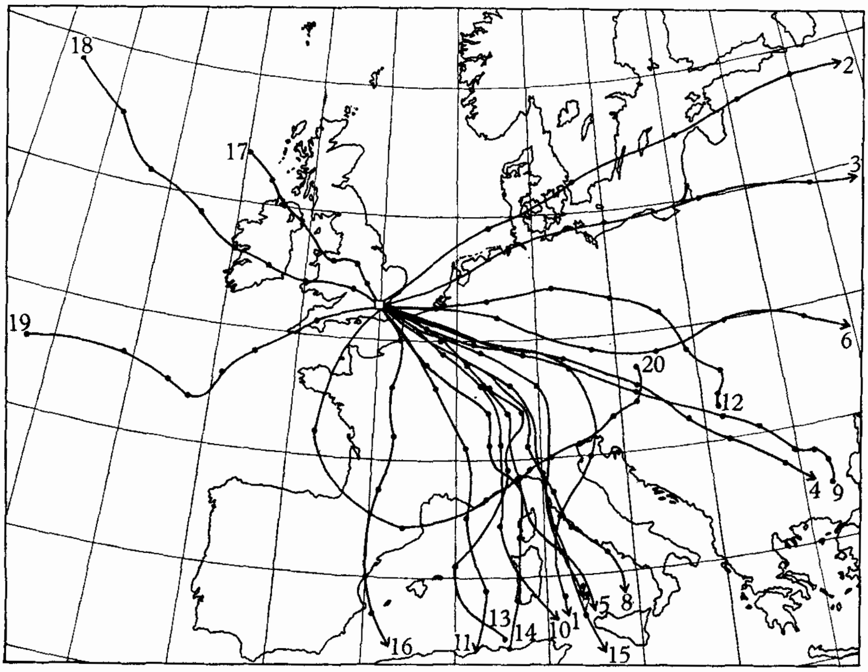

FIGURE 2. Daily trajectories, 1–20 Feb. 1948 at 700 mb.

true wind trajectories. It is hoped such studies as are given in this paper may enable the fundamental characteristics of large-scale turbulence to be more clearly understood. For that reason we have included the summarized data concerning the trajectories in an appendix so that they may be available to other workers.

The purpose of this paper is to discuss the distribution of the end-points of air trajectories initiated at regular intervals i at a point above the earth's surface and pursued for a given length of time t. It is clear that the distribution is related, not only to the time during which the trajectories are pursued, but also to the length of the period T over which they are regularly initiated. Thus there are three time scales, but if N is the number of trajectories followed $(N-1)\,i = T$ and provided N is reasonably large for a given i, the plume can be considered fairly representative of the wind régime and so the magnitude of i does not appear to be significant to the same extent as that of t and T. It is clear that the value of T is of importance in relation to the general pattern of the wind régime prevailing during the period when the trajectories are being drawn. This is at once apparent in the comparison of figures 1*a* and 1*b* which are drawn at 700 mb over North America where data for a large area are most complete. In the former case the general circulation was strong and uniform, in the latter there was much greater meandering of the trajectories and greater variability of the individual winds. The effect is not necessarily seasonal, but it can readily be seen to be dependent on the frequency and type of eddies (depressions and anticyclones) which were passing during the period. For instance, if numerous centres of disturbances were passing over the neighbourhood of the initiation point the plume would have greater spread than if the centres of depressions were following a track to the north. Another pair of plumes is shown in figures 2 and 3 also initiated at 700 mb. In these cases the date of the individual trajectories is indicated by a figure at the end.

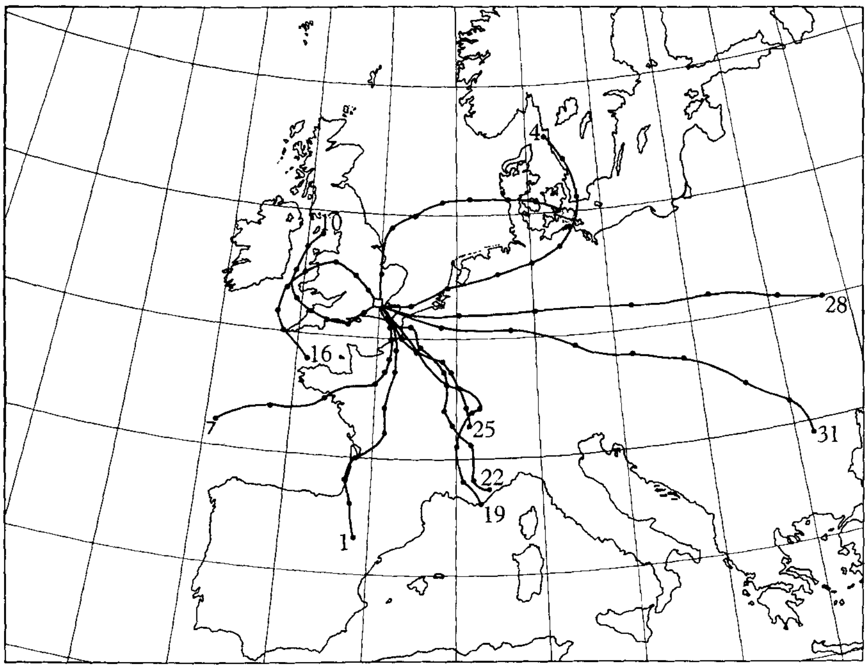

FIGURE 3. Trajectories starting every third day, July 1949 at 700 mb.

The expression of S as a power of the distance of the mean end-point

By a purely empirical approach, the standard vector deviation of the end-points of the trajectories can be related to the magnitude of the mean vector position $[\mathbf{x}]$ of the end-points. The formula used here is the power law

$$S = CL\,|[\mathbf{x}/L]|^a, \tag{1}^*$$

where L is a length which is constant for any one type of trajectory and C and a are arbitrary constants. By introducing the length L, the constant C becomes

* The square brackets indicate an average over the set of N trajectories, or, equivalently, over the period of initiation T.

non-dimensional; however, it varies according to the value selected for L, being proportional to L^{a-1}.

For numerical work, L is taken to be 1 km, and this value will be assumed henceforth unless otherwise indicated. Regression equations were formed of $\log S$ on $\log |[\mathbf{x}]|$, for various time intervals up to 24 or 36 h, for the 27 cases set out in Appendix I. The correlation coefficients were very high, being 0·94 or over in all cases and 0·99 or over in 25 out of the 27 cases, but not too much weight can be attached to such values when the logarithms of numbers are being correlated. The value of a varied from 0·53 to 1·21 with an average of 0·870. It is curious that this value agrees closely with the value 0·875 deduced by Sutton (1953, p. 287) for the very different case of diffusion near the earth's surface in conditions of neutral equilibrium. The values of C varied with the period of initiation—3 months, 1 month, 2 weeks or 24 h as the case might be; more will be said of this below.

On quite a different scale there are some rather similar data available from series of smoke puffs fired from an aircraft above a camera obscura, as described by Durst (1948). These puffs were plotted in the camera obscura with trajectories lasting 1 min or $1\frac{1}{2}$ min; the period of initiation was generally $\frac{3}{4}$–1 h. From these trajectories a plume could be made up in just the same way as is shown in figure 1 and standard vector deviations of the end-points of these trajectories were found after various time intervals. Ten such families of trajectories were worked up; the mean value of a was 0·926, and that of C was 0·15.

A further collection of wind observations obtained from smoke puffs at various heights has been discussed by R. F. Jones (unpublished). Trajectories were initiated over half-hourly periods and the value of C found was 0·06 if we assume arbitrarily that the index a is 0·87.

In addition, Sutton (1932) made an estimate of the value of C from the dispersion of balloons described by Richardson & Proctor (1925). They were released over about 3 h and the value of C was 0·22 corresponding with an assumed value for a of 0·875.

Summary of values of C, a and T

The values of C derived from all the observations mentioned above have been collected together in table 1 and classified according to the period of initiation T.

The modal values of C are put in parentheses when they can be derived. The modal value of a for all the geostrophic trajectories combined is 0·878 and for the 10 smoke puffs is 0·95.

The logarithm of the period of initiation T is plotted against the logarithm of the mean value of C in figure 4. The correlation coefficient between $\log T$ and $\log C$ is 0·85, and the regression equation is

$$\log C = 0{\cdot}487 \log T - 2{\cdot}535, \tag{2}$$

whence to a close approximation $C = 0{\cdot}003 T^{\frac{1}{2}}$, where T is in seconds, or $C = 0{\cdot}18 T^{\frac{1}{2}}$, where T is in hours.

In these calculations, the length L as already explained has been taken as 1 km, but it is a simple matter to convert the constant C to the appropriate value for any other length; for example, if a is 0·87 and L is 10 km, the above values of C

must be multiplied by the factor 0·75; if L is 100 km, the factor is 0·56, and if L is 3000 km the factor is 0·37. It has been suggested that L might suitably be the radius of the earth, since geostrophic trajectories often extend over distances of this order within a few days. More probably perhaps L should be related to the characteristic size of the larger eddies concerned, say about 1000 km for the geostrophic trajectories considered, but only a few kilometres for the smoke puffs. However, this matter has not been pursued further.

Type of observation	Period of initiation (T)	Duration of trajectories	No. of cases	Mean value of a	Value of C ($L = 1$ km)
Geostrophic trajectories	91–92 days	36 h	2	0·865	7·67
	47 days	36 h	1	0·815	5·40
	28–31 days	36 h	8	0·844	(8·36)
	15–20 days	36 h	8	0·909	(2·23)
	24 h	24 h	8	0·848	(1·43)
Richardson's balloons	5 h	—	—	—	0·22
Smoke puffs	$\frac{3}{4}$ h	1 min	10	0·926	(0·12)
	$\frac{1}{2}$ h	—	—	—	0·06

TABLE 1. Mean values of a and C arranged according to the duration of the period of initiation T

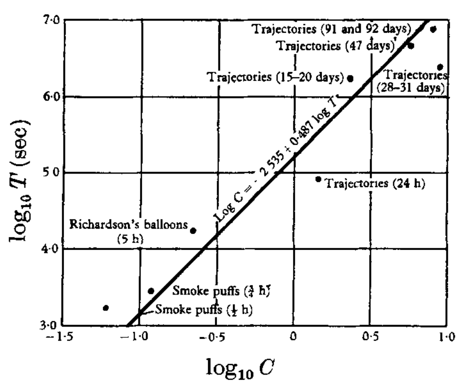

FIGURE 4. Relationship between log C and log T.

Theory

We wish to express the dispersion of the end-points of a series of trajectories, each of which has been followed for a time t from their common point of initiation, as a function of time and of the standard vector deviation of wind during the period of initiation of the trajectories. Let us suppose that a large number N of trajectories be drawn at regular intervals of time $T/(N-1)$ from a particular point in the earth's atmosphere. After an interval of t h, a typical trajectory has extended to a point with position vector $\mathbf{x}$ relative to the point of origin. Let $\mathbf{V}$ be the vector wind at any point on the trajectory. Then by vector summation

$$\mathbf{x} = \int_0^t \mathbf{V}\,dt. \tag{3}$$

Further, if we average over the N trajectories, and subtract from (3), we get

$$\mathbf{x}-[\mathbf{x}] = \int_0^t (\mathbf{V}-[\mathbf{V}])\,dt = \int_0^t \mathbf{v}\,dt, \tag{4}$$

where $\mathbf{v}$ is the vector departure from mean. That is, the vector departure from the mean of the trajectory ends can be obtained from the integral with time of the vector departure from the mean of the wind. Moreover, if S is the standard vector deviation of the end-point of the trajectories at time t after initiation,

$$S^2 = [(\mathbf{x}-[\mathbf{x}])^2] = \left[\int_0^t \int_0^t \mathbf{v}(a).\mathbf{v}(b)\,da\,db\right]. \tag{5}$$

If we assume $\mathbf{v}(t)$ to be a stationary random function of t, and write σ for the standard vector deviation of wind in the period T, i.e.

$$\sigma^2 = [\mathbf{v}(a)]^2 = [\mathbf{v}(b)]^2,$$

equation (5) becomes

$$S^2 = 2\sigma^2 \int_0^t da \int_0^a r(a-b)\,db, \tag{6}$$

where $0 \leqslant a \leqslant t$, $0 \leqslant b \leqslant t$ and $r(a-b)$ is the stretch vector correlation coefficient (Durst 1954) between $\mathbf{v}(a)$ and $\mathbf{v}(b)$. Since $r(a-b)$ is an even function, it may be shown that (6) is equivalent to

$$S^2 = 2\sigma^2 \int_0^t \int_0^{\xi'} r(\xi)\,d\xi\,d\xi', \tag{7}$$

an expression which is of the same form as that given by Taylor (1921) for diffusion parallel to a fixed axis. In order to discuss S in terms of σ we need therefore to know the behaviour of $r(t)$.

It is convenient to note here that

$$[\{\mathbf{V}(a)-\mathbf{V}(b)\}^2] = [\{\mathbf{v}(a)-\mathbf{v}(b)\}^2] = 2\sigma^2 - 2\sigma^2 r(a-b), \tag{8}$$

provided $[\mathbf{V}(a)] = [\mathbf{V}(b)]$.

The form of $r(t)$

Large-scale diffusion in the free air is controlled by the largest eddies, which in middle latitudes consist of travelling cyclones and anticyclones and the general long-wave pattern. The eddies in the free atmosphere that are concerned in any long period of diffusion may indeed be of various sizes, but their average size does not change with time in any systematic way. Taylor (1921) and others have considered the applicability of an exponential form for the Lagrangian correlation coefficient $r(t)$; in particular, Brunt (1941) argues that it holds when the eddies are all of one size. The rough constancy of the size distribution of the largest atmospheric eddies then suggests that for large-scale diffusion the form of $r(t)$ might well approximate to the exponential,

$$r(t) = e^{-\alpha t}, \tag{9}$$

in which $1/\alpha$ may be looked on as the characteristic time of those eddies which have the major effect on the motion of a particle. These eddies contain the principal part of the energy and play an important part in determining the wind fluctuation at a fixed point (σ) and the eddy viscosity at a fixed point (K). The latter is to be regarded in the present context as the coefficient of eddy viscosity of lateral mixing. Moreover, σ^2/K has the same dimensions as α, and evidence will be produced that they are approximately equal, so that

$$r(t) \doteqdot e^{-\sigma^2 t/K}. \tag{10}$$

It is worth noting that in the sequel we find that, for geostrophic trajectories in the upper air, $1/\alpha$ is of the order of 24 h which is the time scale that would be expected from the passage of the large-scale atmospheric disturbances.

It is important to realize that for testing the form of $r(t)$ measurements must be made within ranges which are rather strictly confined. It has been pointed out by Taylor that when t is small and $r(t)$ is nearly unity, then S is initially nearly σt; also that if $r(t)$ is effectively zero for all $t \geqslant t_1$, $\int_0^t r(\xi)\,d\xi$ tends to a finite limit as t increases and consequently S varies as $t^{\frac{1}{2}}$ when t is much greater than t_1, no matter what the form of $r(t)$ is for values of t less than t_1. More precisely, we have for $t \geqslant t_1$,

$$S^2(t) \approx k(t-t_1)+S^2(t_1), \tag{11}$$

where $k = 2\sigma^2 \int_0^\infty r(\xi)\,d\xi$ is a constant. This gives a simple formula for diffusion for times exceeding t_1 and incidentally shows clearly that if we wish to examine the form of $r(t)$, it will not help if we extend the time during which the samples are followed much beyond this critical time t_1. In the case of geostrophic trajectories in the free air the critical time t_1 would appear to be about 36 h but for the surface trajectories about 18 h.

However, if we assume that $r(t)$ is exponential in form we can calculate the dispersion of the end-points of the trajectories after they have been followed for a given time t by use of (7), which on integration gives

$$\frac{S^2}{\sigma^2} = \frac{2}{\alpha^2}(\alpha t - 1 + e^{-\alpha t}) \tag{12}$$

and the values of S can then be compared with data such as those given in Appendix I.

For times greater than t_1, the exponential term in the preceding equation may be neglected; this leads to an approximation to the value of α in the form

$$\alpha = 2\sigma^2 \frac{t-t_1}{S^2-S_1^2} \quad (t > t_1). \tag{13}$$

If we now put $\alpha = \sigma^2/K$, the eddy viscosity for lateral mixing (K) is seen to be obtainable from the spread of the end-points of the trajectories; K does not depend explicitly on the standard deviation of the wind.

Magnitude of errors involved in using geostrophic trajectories

Before proceeding to the discussion of the results a word must be said as to the errors likely to arise in taking the geostrophic trajectories as representative of the true motion of the atmosphere. The principal causes of error are inaccuracy in measurement of geostrophic winds and the inherent unrepresentativeness of the geostrophic wind as a picture of the true air flow. The magnitude of these errors over the British Isles is given by Murray (1954) and a note on their effects on trajectories by Durst & Davis (1957).

Let the true wind be $\mathbf{V}+\mathbf{v}$ and the error in its measurement be $\boldsymbol{\epsilon}$; then the calculated correlation coefficient between $\mathbf{v}(a)$ and $\mathbf{v}(b)$ becomes

$$r' = \frac{[\{\mathbf{v}(a)+\boldsymbol{\epsilon}_1\}\{\mathbf{v}(b)+\boldsymbol{\epsilon}_2\}]}{\sigma^2+[\boldsymbol{\epsilon}^2]},$$

instead of the true value $[\mathbf{v}(a)\,\mathbf{v}(b)]/\sigma^2$. Moreover, if we can assume there is little or no correlation between $\boldsymbol{\epsilon}_1$ and $\boldsymbol{\epsilon}_2$ or between $\boldsymbol{\epsilon}$ and $\mathbf{v}$ except very near time $t=0$, then

$$r' = \frac{[\mathbf{v}(a)\,\mathbf{v}(b)]}{\sigma^2+[\boldsymbol{\epsilon}^2]}.$$

If $[\boldsymbol{\epsilon}^2]$ is small in comparison with σ^2 we get

$$r-r' = [\boldsymbol{\epsilon}^2]\,r/\sigma^2.$$

If we go back to equation (7), and use the value of σ^2 deduced from the actual measurements of velocities (i.e. if we really use $\sigma^2+[\boldsymbol{\epsilon}^2]$), we see that $\sigma^2+[\boldsymbol{\epsilon}^2]$ occurs in both numerator and denominator, and in consequence there is no consistent error in S due to errors in the measurements of velocities.

It is true that a large value of $\boldsymbol{\epsilon}_1$ will lead to the apparent trajectory running away from the true trajectory with in consequence a large value of $\boldsymbol{\epsilon}_2$. This effect is discussed by Durst and Davis (1957). After 36 h the results of this effect might produce an error of 250–350 km for individual trajectories at 700 mb, and when one looks at the magnitude of the standard deviation of end-points given in Appendix I it is clear that an error of such an amount may on some occasions produce an effect which is an appreciable proportion of the true S. However, on the whole the error involved in using geostrophic trajectories in determining the values of S is probably not more than 10 %, at any rate for trajectories extending to 36 or 48 h.

Values of the correlation coefficient $r(t)$

The values of $r(t)$ have been evaluated from three types of data: (a) from a series of constant level balloons which were flown at 300 mb for periods of 2, 3 or 4 days (Mastenbrook & Anderson 1953); (b) from a considerable series of geostrophic trajectories at levels of 500 and 700 mb; and (c) from surface charts. The values from the constant level balloons are set out in Table 2, those of the geostrophic trajectories in Table 3.

(a) *Derivation from constant level balloons*

In table 2 the value of $r(t)$ has been calculated from the mean square differences between observed velocities at each time interval by means of equation (8). By proceeding in this way it was possible to obtain a considerable number of comparisons from a limited number of trajectories. The correlation coefficients nearly follow an exponential law and values of α have been calculated on the assumption that $r(t)$ is of the form $e^{-\alpha t}$.

There is, however, a difficulty in that there are errors in the positioning of the balloons which are stated to range from 20 miles in the case of good fixes to 40 miles in the case of moderately good fixes and up to 60 miles in the case of poor fixes. From internal evidence, however, it is clear that these figures are excessively high, and although any correction for position error will tend to increase all the correlation coefficients, the resulting increase in the value of K would be hardly significant.

		2	4	6	8	10	12	14
Time interval (h) (t)		2	4	6	8	10	12	14
No. of pairs of observations		59	51	43	35	31	27	24
Standard differences (knots)	N.–S.	19	22	28	30	33	38	39
	E.–W.	17	19	22	25	28	30	32
	Vector	26	29	35	39	43	49	50
$r(t)$		0·72	0·66	0·50	0·38	0·24	0·02	−0·02
$\alpha \times 10^5\,\mathrm{sec}^{-1}$		4·5	2·9	3·2	3·4	3·9	—	—

$\sigma = 35\,\mathrm{kt}$, mean $\alpha = 3{\cdot}6 \times 10^{-5}\,\mathrm{sec}^{-1} = 0{\cdot}13\,\mathrm{h}^{-1}$, $K = \alpha/\sigma^2 = 9{\cdot}3 \times 10^{10}\,\mathrm{cm}^2\,\mathrm{sec}^{-1}$.

TABLE 2. Values of $r(t)$ derived from constant level balloons flown at 300 mb over America and the North Atlantic in latitudes north of 40° N

(*b*) *Derivation from geostrophic trajectories at* 700 *and* 500 *mb*

For a number of groups of geostrophic trajectories the winds have been tabulated after each time interval and the actual correlation coefficients between the velocity at one time and that at a subsequent time on the same trajectory have been calculated. In table 3 there are given the correlation coefficients between measured geostrophic winds at one time and at the appropriate point on the same trajectory at a subsequent time. The number of trajectories on which they are based is given. On each trajectory a number of pairs of points can be taken with the same time interval so that the correlation coefficients are based on several times as many pairs as the number of trajectories, the number of pairs being entered in parentheses in the table. Correlation coefficients are given separately for the south–north direction (S) and the west–east direction (W) and a vector correlation coefficient is also calculated and entered below the others. In October and November 1949, each month was split up into six periods of 5 days and departures from 5-day means were formed so that the average correlation coefficients were calculated for 5-day periods of initiation. Some specimens of the relationship between $\log_{10} r(t)$ and t are shown in figure 5.

The logarithms of the mean stretch-vector correlation coefficients entered in table 3 have been plotted in figure 6; these lie on a straight line and so fit a relationship such that

$$r(t) = e^{-\alpha t},$$

where $\alpha = 1{\cdot}13 \times 10^{-5}\,\mathrm{sec}^{-1}$ or $0{\cdot}041\,\mathrm{h}^{-1}$.

If, then, $\alpha = \sigma^2/K$ and $\sigma = 17{\cdot}6$ knots

$$K = 7{\cdot}2 \times 10^{10}\,\mathrm{cm}^2\,\mathrm{sec}^{-1}.$$

The exponential form of $r(t)$ has also been applied by Solot & Darling (1958)

Date	Height (mb)	No. of trajectories	Standard deviation (kt) of first 36 h S.	W.	Time interval 6 h S.	W.	12 h S.	W.	18 h S.	W.	24 h S.	W.	30 h S.	W.	36 h S.	W.	42 h S.	W.	48 h S.	W.
1–20 Feb. 1948	700	20	19·5	21·5	0·696	0·797	0·539	0·513	0·402	0·487	0·366	0·522	0·326	0·435	0·262	0·346	—	—	—	—
			29·0		0·745 (240)		0·517 (200)		0·437 (160)		0·428 (120)		0·364 (80)		0·299 (40)					
17 Apr.–4 May 1950	700	16	10·0	11·7	0·723	0·779	0·577	0·628	0·369	0·440	0·262	0·350	0·100	0·282	0·076	0·295	0·020	0·386	—	—
			15·4		0·777 (224)		0·609 (192)		0·409 (160)		0·314 (128)		0·210 (96)		0·210 (64)		0·246 (32)			
5–20 May 1950	700	16	6·1	6·8	0·731	0·700	0·709	0·520	0·500	0·457	0·428	0·420	0·271	0·438	0·302	0·381	0·140	0·183	—	—
			9·2		0·715 (224)		0·560 (192)		0·477 (160)		0·423 (128)		0·362 (96)		0·345 (64)		0·162 (32)			
1–15 June 1950	700	15	6·2	9·3	0·666	0·828	0·463	0·750	0·326	0·607	0·304	0·505	0·232	0·500	0·262	0·337	0·276	0·139	—	—
			11·2		0·785 (210)		0·663 (180)		0·512 (150)		0·443 (120)		0·416 (90)		0·310 (60)		0·377 (30)			
17 Apr.–15 June 1950	700	47	7·8	9·5	0·721	0·785	0·575	0·652	0·368	0·496	0·329	0·411	0·190	0·376	0·191	0·326	0·129	0·295	—	—
			12·3		0·760 (658)		0·621 (564)		0·477 (470)		0·380 (376)		0·303 (282)		0·272 (188)		0·227 (94)			
Oct. 1949	500	30	21·2	18·1	—	—	0·600	0·408	—	—	0·356	0·230	—	—	−0·013	0·148	—	—	−0·422	0·109
			27·9				0·490 (120)				0·275 (90)				0·057 (60)				−0·150 (30)	
Nov. 1949	500	30	13·3	18·0	—	—	0·468	0·784	—	—	0·257	0·641	—	—	0·154	0·392	—	—	−0·057	0·156
			22·4				0·671 (120)				0·499 (90)				0·293 60)				0·055 (30)	
Apr. 1948	700	15	11·5	12·8	—	—	0·560	0·651	—	—	0·219	0·472	—	—	−0·115	0·284	—	—	−0·582	0·249
			17·3				0·613 (60)				0·369 (45)				0·095 (30)				−0·075 (15)	
May 1948	700	16	11·1	12·1	—	—	0·615	0·607	—	—	0·221	0·238	—	—	0·079	0·173	—	—	−0·009	0·080
			16·4				0·610 (72)				0·229 (48)				0·126 (32)				0·037 (16)	
June 1948	700	15	8·2	8·8	—	—	0·723	0·737	—	—	0·540	0·524	—	—	0·336	0·206	—	—	0·535	0·195
			12·2				0·725 (60)				0·528 (45)				0·262 (30)				0·328 (15)	
Apr., May, June 1948	700	46	10·7	12·8	—	—	0·620	0·719	—	—	0·299	0·518	—	—	0·029	0·420	—	—	−0·110	0·390
			16·7				0·680 (192)				0·433 (138)				0·266 (92)				0·188 (46)	
1–15 Nov. 1947	700	30	13·0	9·2	—	—	0·782	0·638	—	—	0·529	0·516	—	—	0·403	0·453	—	—	0·214	0·324
			15·9				0·723 (120)				0·521 (90)				0·415 (60)				0·244 (30)	
1–15 Apr. 1947	700	30	6·6	4·2	—	—	0·464	0·412	—	—	0·410	0·319	—	—	0·498	0·362	—	—	0·035	0·440
			7·8				0·445 (120)				0·273 (90)				0·430 (60)				0·290 (30)	
		R.M.S.	17·6		Mean (logarithmic)		0·604		—	—	0·381		—	—	0·228		—	—	—	
5-day periods																				
Oct. 1949	500	30	13·1	12·2	—	—	0·336	0·168	—	—	0·135	0·060	—	—	−0·117	−0·021	—	—	−0·380	0·132
			17·9				0·251 (120)				0·118 (90)				−0·072 (60)				−0·162 (30)	
Nov. 1949	500	30	10·5	12·2	—	—	0·378	0·680	—	—	0·149	0·441	—	—	0·193	0·392	—	—	−0·006	0·315
			16·1				0·554 (120)				0·312 (90)				0·324 (60)				0·207 (30)	

TABLE 3. Values of $r(t)$ derived from geostrophic trajectories

to the same problem of the spread of end-points of trajectories in the free atmosphere; the value taken for α corresponds with $0{\cdot}038\,\mathrm{h}^{-1}$, in good agreement with the value found above.

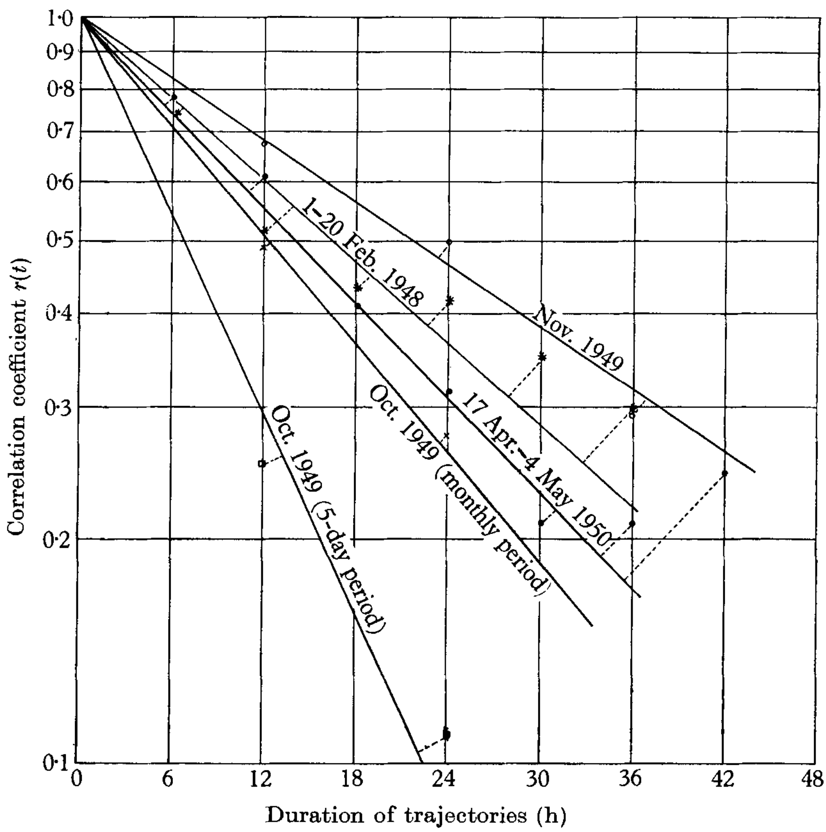

FIGURE 5. Relation between correlation coefficient, $r(t)$, and the duration of each trajectory, t.

(c) *Derivation from geostrophic trajectories at the surface*

From 1943 to 1946 a very close network of meteorological stations was maintained over the British Isles, and observations were plotted at 3 h intervals. Surface geostrophic trajectories were drawn from two points over the British Isles on 8 days chosen at random. These trajectories were pursued for 24 h and new ones initiated every 3 h (nine times in all) so that the period of initiation of each family of trajectories was 24 h. The winds were measured every 3 h and correlation coefficients were calculated for 6, 12, 18 and 24 h intervals from the eighteen comparisons for each family. The results are set out in table 4.

The values of α at the foot of table 4 are derived from the exponential form (9) for $r(t)$, and the value of K follows from $K = \sigma^2/\alpha$. In Appendix I there are set out the standard vector deviations of the end-points after the trajectories had been followed for various times and also the vector mean distance that the end-points had reached during those times.

In table 5 values of α and K are set out which have been derived in three independent ways. First in columns 7 they have been derived by the direct calculation of correlation coefficients from the velocities at various intervals of time. These coefficients given in tables 3 and 4 have been fitted to an exponential function from which α has been derived and hence K. Secondly, in the columns 8,

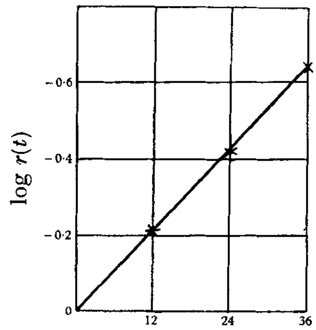

FIGURE 6. Mean value of $\log r(t)$ as function of t.

Date	No. of trajectories	Standard vector deviation (kt)	Time interval (h) 6	12	18	24
21–22 Sept. 1943	18	11·3	0·27	0·04	0·02	−0·06
25–26 Sept. 1943	18	7·7	0·43	0·59	0·10	0·21
3–4 March 1944	18	8·7	0·18	−0·08	0·01	0·13
6–7 March 1944	18	6·9	0·16	0·02	0·18	0·01
16–17 June 1944	18	12·9	0·56	0·14	0·07	−0·33
22–23 June 1944	18	6·9	0·36	−0·29	−0·59	−0·55
12–13 Dec. 1946	18	4·9	0·19	−0·04	0·17	−0·16
16–17 Dec. 1946	18	8·7	0·09	0·07	0·35	0·33
Mean	—	8·5	0·28	0·06	0·04	−0·05
$\alpha \times 10^5\,\text{sec}^{-1}$	—	—	6·1	6·4	5·0	—
Mean K				$3{\cdot}3 \times 10^9\,\text{cm}^2\,\text{sec}^{-1}$		

TABLE 4. Vector correlation coefficients from surface geostrophic trajectories over the British Isles

the values of S/σ have been calculated from the data in Appendix I for various values of t up to 36 h for the trajectories in each group at 300, 500 and 700 mb. and up to 18 h for the surface trajectories. These have been plotted on diagrams such as figure 7 and the value of α was chosen for which the plots of S/σ gave the best fit, and again K was appropriately calculated. Figure 8 shows some specimens of the fits. Thirdly, in columns 9 the value of K has been calculated from the data in Appendix I by the use of equation (13) and the relation $\alpha = \sigma^2/K$. In these calculations t_1 was chosen to be 36 h in the upper air groups and 18 h in the surface trajectories, while t was taken as the biggest value available, which was 72 h in many cases.

Thus there were two, and in some cases three, estimates of α and K; in the case of columns 7 and 9 they were derived by quite different methods and from

(1)	(2)	(3)	(4)		(5)		(6)		(7)		(8)		(9)	
					Standard deviation vector of wind (σ)				Coefficient of eddy diffusivity for lateral mixing					
		Period of initiation	Average velocity over 36 h		(a) At point of initiation		(b) From all points up to 36 h		Derived from correlation coefficients		Derived from end-points of trajectories (0 to 36 h)		Derived from end-points of trajectories by $K=S^2-S_1^2/2(t-t_1)$	
Date	Height (mb)	(days)	kt	m/s	kt	m/s	kt	m/s	α (h^{-1})	K ($=\sigma^2/\alpha$) (cm^2/sec)	α (h^{-1})	K ($=\sigma^2/\alpha$) (cm^2/sec)	α ($=\sigma^2/K$) (h^{-1})	K (cm^2/sec)
Apr.–June 1948	700	91	7	3·6	17	8·9	17	8·6	0·035	$7·6\times10^{10}$	0·05	6×10^{10}	0·033	$8·0\times10^{10}$
Oct.–Dec. 1949	500	92	20	10·3	28	14·4	—	—	—	—	0·05	15×10^{10}	0·071	$10·5\times10^{10}$
17 Apr.–15 June 1950	700	47	9	4·6	14	7·2	12	6·3	0·040	$3·6\times10^{10}$	0·05	4×10^{10}	0·029	$5·0\times10^{10}$
Apr. 1948	700	30	14	7·0	19	9·8	17	8·9	0·049	$5·8\times10^{10}$	0·07	4×10^{10}	0·041	$7·0\times10^{10}$
May 1948	700	31	6	3·1	15	7·7	16	8·4	0·053	$4·8\times10^{10}$	0·03	8×10^{10}	0·057	$4·5\times10^{10}$
June 1948	700	30	3	1·3	11	5·5	12	6·4	0·030	$4·9\times10^{10}$	0·02	7×10^{10}	0·027	$5·5\times10^{10}$
Oct. 1949	500	31	25	12·6	33	16·9	28	14·4	0·064	$11·6\times10^{10}$	0·03	2×10^{10}	0·071	$10·5\times10^{10}$
Nov. 1949	500	30	13	6·9	27	14·0	22	11·5	0·032	$14·8\times10^{10}$	0·07	7×10^{10}	0·041	$11·5\times10^{10}$
Dec. 1949	500	31	21	10·8	21	10·5	—	—	—	—	0·06	7×10^{10}	0·034	$12·0\times10^{10}$
July 1949	700	20	8	4·2	14	7·4	—	—	—	—	0·01	2×10^{10}	—	—
Aug. 1949	700	20	13	6·8	21	10·6	—	—	—	—	0·04	10×10^{10}	—	—
Feb. 1948	700	20	23	12·0	24	12·1	29	14·9	0·042	$19·0\times10^{10}$	0·06	13×10^{10}	—	—
17 Apr.–4 May 1950	700	16	10	4·9	16	8·1	15	7·9	0·046	$4·7\times10^{10}$	0·04	6×10^{10}	0·035	$6·5\times10^{10}$
5–20 May 1950	700	16	9	4·8	10	5·1	9	4·7	0·041	$1·9\times10^{10}$	0·06	1×10^{10}	0·027	$3·0\times10^{10}$
1–15 June 1950	700	15	8	3·9	11	5·4	11	5·8	0·034	$3·5\times10^{10}$	0·05	2×10^{10}	0·022	$5·5\times10^{10}$
1–15 Aug. 1947	700	15	13	6·8	9	4·8	8	4·0	0·039	$1·5\times10^{10}$	0·01	6×10^{10}	0·015	$3·9\times10^{10}$
1–15 Nov. 1947	700	15	17	8·5	15	7·9	16	8·2	0·027	$9·0\times10^{10}$	0·02	12×10^{10}	0·040	$6·0\times10^{10}$
July 1947	300	30	21	11·0	38	19·6	—	—	—	—	0·10	14×10^{10}	0·141	$9·8\times10^{10}$
Feb. 1948	300	28	25	13·0	45	22·9	—	—	—	—	0·15	13×10^{10}	0·151	$12·5\times10^{10}$
Oct. 1949	500	5	—	—	—	—	18	9·2	0·070	$4·4\times10^{10}$	—	—	—	—
Nov. 1949	500	5	—	—	—	—	16	8·3	0·043	$5·8\times10^{10}$	—	—	—	—
		(h)	Over 24 h				Up to 24 h				(0–18 h)		(18–24 h)	
21–22 Sept. 1943	Surface	24	15	7·8	10	5·0	11	5·8	—	—	0·15	8×10^{9}	0·12	10×10^{9}
25–26 Sept. 1943	Surface	24	14	7·1	8	4·1	8	3·9	—	—	0·10	5×10^{9}	0·55	1×10^{9}
3–4 Mar. 1944	Surface	24	18	9·2	6	2·9	9	4·4	—	—	0·20	3×10^{9}	0·10	7×10^{9}
6–7 Mar. 1944	Surface	24	11	5·7	4	1·9	7	3·5	—	—	0·35	1×10^{9}	0·22	2×10^{9}
16–17 June 1944	Surface	24	13	6·4	14	7·0	13	6·6	—	—	0·10	16×10^{9}	0·11	14×10^{9}
22–23 June 1944	Surface	24	8	4·0	5	2·6	7	3·5	—	—	0·50	$0·7\times10^{9}$	0·44	1×10^{9}
12–13 Dec. 1946	Surface	24	13	6·8	3	1·6	5	2·5	—	—	0·75	$0·3\times10^{9}$	0·22	1×10^{9}
16–17 Dec. 1946	Surface	24	13	6·8	5	2·4	9	4·4	—	—	0·30	2×10^{9}	0·10	7×10^{9}

Note. The values of K in columns 7 and 8 have been derived from $K=\sigma^2/\alpha$, where σ is the standard deviation taken from column 6 when available, and otherwise from column 5. The value of α in column 9 has been derived from $\alpha=\sigma^2/K$.

TABLE 5. Values of α and K deduced from the geostrophic trajectories by various methods

different portions of the trajectories, and in the case of columns 8 and 9 they were derived by somewhat the same method (i.e. by the assumption before integration that $r(t)$ followed an exponential law) but the measurements were made at different parts of the trajectories.

The agreement between the values of K is closer than that between the values of α, the correlation coefficient between the values of columns 7 and 9 being 0·92

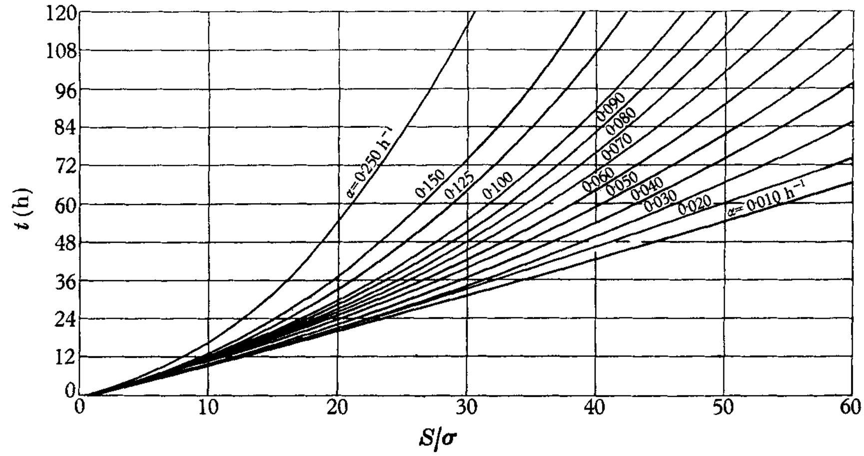

FIGURE 7. Values of ratio S/σ for various values of α and t.

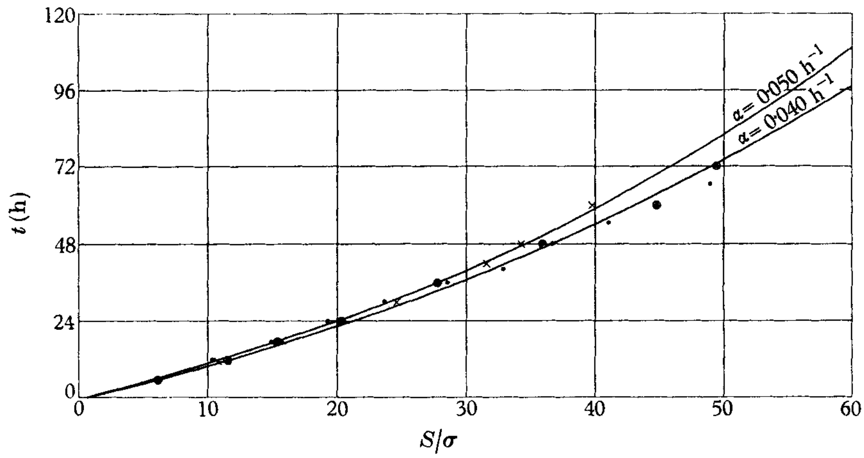

FIGURE 8. Illustration of method of deducing α from the relationship of S/σ to t. ●, 17 Apr.–15 June 1950; ⊙, Apr.–June 1948; ×, Oct.–Dec. 1949.

in the case of K and 0·64 in the case of α. In figure 9 is shown a dot diagram illustrating the relationship of the values of α and K given in column 9 with those given in column 7.

The agreement is sufficiently good to give confidence that the variations in the values of α and K are not due to casual errors. The means of the 12 available pairs of values of K are 6·1 and $6{\cdot}4\times10^{10}\,\mathrm{cm^2\,sec^{-1}}$ for columns 7 and 9 respectively; the corresponding mean values of α are 0·041 and $0{\cdot}037\,\mathrm{h^{-1}}$.

In table 6 there are set out the best values of σ, α and K that can be deduced from table 5. σ is taken from column 6 of that table when possible, otherwise from column 5, and α and K are derived from the average of columns 7 and 9 (or from 8 if neither 7 nor 9 was available).

At the higher levels where the standard deviation of wind is in general greater there is clearly a tendency for both α and K to be greater. In figure 10 there is shown the relationship between K and σ; the observations at different pressure levels are indicated by various symbols.

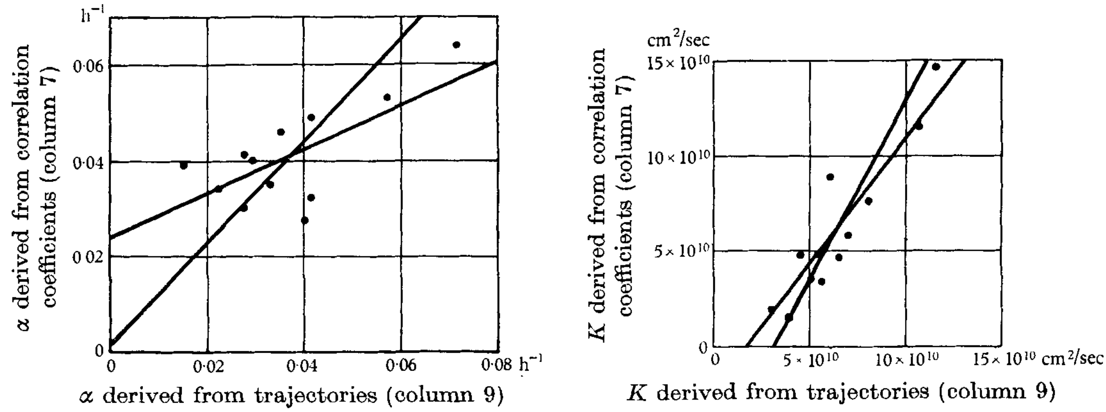

FIGURE 9. Comparison of values of α and K derived by two independent methods (see table 5).

On the diagram have also been put crosses at points representing the mean value of K against σ for tables 2 and 3. That for table 3 fits the regression line; that for table 2 (constant level balloons) is in agreement with the two 300 mb groups of geostrophic trajectories.

The relationship between K and σ for the 19 cases with observations at 500 and 700 mb is shown in figure 10, the regression of K on σ being given by

$$K = (1{\cdot}12\sigma - 2{\cdot}8)\,10^{10}\,\mathrm{cm^2\,sec^{-1}}.$$

K, however, is not in general a function of σ alone. If α were constant, K would be proportional to σ^2. On the other hand, K may be regarded as the product of eddy velocity (σ) and characteristic eddy size (σ/α), so that if the size is constant then K is proportional to σ. No doubt the truth usually lies somewhere between these two extremes.

It seems from this examination that there is fairly strong evidence that the correlation coefficients between the winds at the end-points of the trajectories follow closely an exponential law, particularly in view of the linearity in the points on figure 6 and of the agreement between the values of α shown in columns 7 and 9 of table 5. Moreover, it seems that K is probably the coefficient of eddy viscosity for lateral mixing. It is of the same order of magnitude as the values deduced by Haurwitz (1941), who quotes 4×10^7 g/cm sec for the exchange coefficient derived from the transport of heat across parallels of latitude. To obtain the corresponding figure for the eddy viscosity we have to divide this quantity by the density, i.e. by 9×10^{-4} g/cm^3 at 700 mb and 7×10^{-4} g/cm^3 at

500 mb, so obtaining 4×10^{10} cm²/sec for 700 mb and 6×10^{10} cm²/sec for 500 mb. Other values of the exchange coefficient have been derived by Lettau (1936) which vary with latitude from $4{\cdot}4 \times 10^7$ g/cm sec in latitude 35° to a maximum of $8{\cdot}2 \times 10^7$ g/cm sec in latitude 50°–55°; these correspond with $K = 5 \times 10^{10}$ and 9×10^{10} cm²/sec respectively.

Date ...	Apr.–June 1948	17 Apr.–15 June 1950	Apr. 1948	May 1948	June 1948	July 1949	Aug. 1949
Pressure (mb)	700	700	700	700	700	700	700
σ (m sec.$^{-1}$)	8·6	6·3	8·9	8·4	6·4	7·4	10·6
α (h$^{-1} \times 10^2$)	3·4	3·5	4·5	5·5	2·9	1·0	4·0
K (cm² sec$^{-1} \times 10^{10}$)	7·8	4·3	6·4	4·7	5·2	2·0	10·0
Period of initiation (days)	91	47	30	31	30	20	20
Date ...	Feb. 1948	17 Apr.–4 May 1950	5–20 May 1950	1–15 June 1950	1–15 Aug. 1947	1–15 Nov. 1947	Oct.–Dec. 1949
Pressure (mb)	700	700	700	700	700	700	500
σ (m sec^{-1})	14·9	7·9	4·7	5·8	4·0	8·2	14·4
α (h$^{-1} \times 10^2$)	4·2	4·1	3·4	2·8	2·7	3·3	7·1
K (cm² sec.$^{-1} \times 10^{10}$)	19·0	5·6	2·5	4·5	2·7	7·5	10·5
Period of initiation (days)	20	16	16	15	15	15	92
Date ...	Oct. 1949	Nov. 1949	Dec. 1949	Oct. 1949	Nov. 1949	July 1947	Feb. 1948
Pressure (mb)	500	500	500	500	500	300	300
σ (m sec^{-1})	14·4	11·5	10·5	9·2	8·3	19·6	22·9
α (h$^{-1} \times 10^2$)	6·7	3·7	3·4	7·0	4·3	14·1	15·1
K (cm² sec$^{-1} \times 10^{10}$)	11·1	13·1	12·0	4·4	5·8	9·8	12·5
Period of initiation (days)	30	30	31	5	5	30	28

TABLE 6. Best values of σ, α and K derived from Table 5

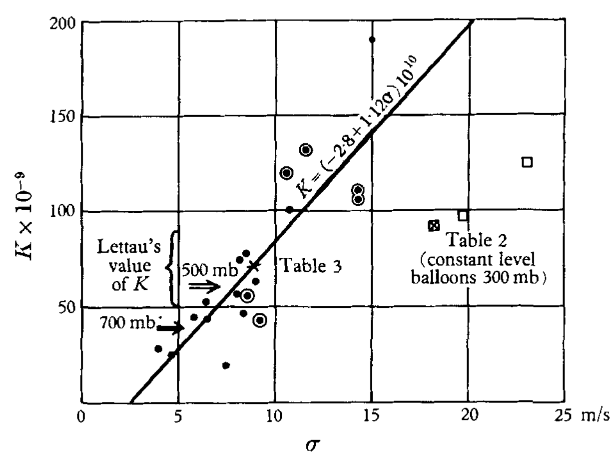

FIGURE 10. Relationship between standard deviation of wind (σ) and K. □, observations at 300 mb; ⊙, observations at 500 mb; •, observations at 700 mb; ×, results from tables 2 and 3; ⇛, Haurwitz's value of K.

The diffusion laws in relation to time scale

From this work it would seem that there is a remarkable agreement between the values of K (interpreted as the coefficient of large-scale horizontal diffusion) which we have found and those derived by other workers by quite different methods. The inference is that the Lagrangian correlation coefficients follow an exponential law. However, the empirical relation between C and T set out above would seem to support the hypothesis that the power law also applies to this type of diffusion.

We believe that both are indeed applicable for short times and that the scheme below sets out in a practical and convenient form the modes of 'diffusion' of the end-points of successive trajectories of duration t.

	$t=0$ small	moderate large	$t \to \infty$
$r(t)$	Near unity	power law *or* exponential law	effectively zero
S.D. of end-points	σt	$CL\left\lvert\frac{[\mathbf{V}]\,t}{L}\right\rvert^{a}$ *or* $\frac{\sqrt{2}\,\sigma}{\alpha}(\alpha t - 1 + e^{-\alpha t})^{\frac{1}{2}}$	$P\sigma t^{\frac{1}{2}}$ *or* $(2Kt)^{\frac{1}{2}}$

Here P is a constant. It may be noted that not only is C a function of T, but σ is also a function of T, as can be seen in Appendix II; therefore C must itself be a function of σ.

Application of results to large-scale diffusion

Instantaneous emission. In this case a 'cloud' is produced instantaneously at the source. The centre of gravity of the cloud travels along a wind trajectory, meanwhile the cloud itself grows by small-scale diffusion. The examination of (geostrophic) trajectories through the source shows the area within which the centre of gravity of the cloud will have arrived after time t from the moment of generation. The most probable position will be that point arrived at by the mean trajectory (the trajectory followed by the mean wind) through the source (e.g. the appropriate monthly mean wind). If the distribution of the trajectory end-points is assumed to be Gaussian and their standard deviation is known, the probability of the centre of gravity of the cloud arriving at any particular point at time t can be set down.

Continuous emission. In this case only a point source need be considered. The particles are emitted as a continuous plume which broadens by small-scale diffusion as it gets further and further (in time) from the source. First, however, we ignore the broadening of the plumes and consider the distribution which results from the variation of the trajectories with time. If the end-points obtained by following each of a succession of trajectories for a time t have a Gaussian distribution, then the mean concentration χ of diffusing substance along a horizontal axis normal to the mean trajectory is given approximately by

$$\chi = \frac{Q}{\pi^{\frac{1}{2}} S\,|[\mathbf{V}]|}\,e^{-y^2/S^2}, \tag{14}$$

where Q is the rate of emission of diffusing substance at the source, S is the standard deviation of the distance of the end-points of the trajectories from their centre of mass, and y is distance from the mean trajectory.

If the broadening of the instantaneous plume by small-scale diffusion is taken into account, it may be remarked that (14) remains valid as a first approximation since the 'coefficient of diffusion' appropriate to the trajectories is several magnitudes greater than the coefficient of small-scale diffusion.

Moreover, S is dependent on the period of initiation in the way that has been discussed for the geostrophic trajectories; hence we can see how the mean plume gradually broadens with time as S increases.

Vertical diffusion. Hitherto only the horizontal spread has been considered. If the coefficient of eddy diffusion in the vertical K_z were known, it would be possible to estimate the vertical spread. Thus for sufficiently large t the standard deviation of the vertical spread is $\sqrt{(2K_z t)}$. Information about the value of K_z in the free atmosphere is scanty; a value of 10^3 or 10^4 cm/sec is appropriate to the friction layer, but in the free atmosphere the value is probably greater, perhaps of the order 10^5 or 10^6, or even more, according to circumstances. After 48 h the standard deviation of the vertical spread would be 0·6, 2 or 6 km according as the value of K_z is 10^4, 10^5 or 10^6 cm/sec and after 8 days would be 1, 4 or 12 km respectively.

It is seen from these figures that if the coefficient of eddy diffusion is no greater in the free atmosphere than it is in the friction layer the diffusing material would have spread out in a flat disk after a week or so, but if the diffusion coefficient is as great as 10^6 it would have spread vertically throughout the troposphere after 1 or 2 days. There is evidently need for further examination of the magnitude of the coefficient of eddy diffusion in the vertical.

When the vertical spread is pronounced, the horizontal distribution of the material may be distorted from the supposed Gaussian form by the effects of wind shear in the vertical.

We acknowledge with thanks the permission to publish this paper given by the Director-General of the Meteorological Office. We also wish to thank Sir Graham Sutton, F.R.S., and Dr F. Pasquill for the interest they have shown in our researches and for the valuable suggestions they have given us.

REFERENCES

Brunt, D. 1941 *Physical and Dynamical Meteorology*, 2nd ed. Cambridge University Press.

Durst, C. S. 1948 *Quart. J. Roy. Met. Soc.* **74**, 349.

Durst, C. S. 1954 *Geophys. Mem., Lond.*, no. 93.

Durst, C. S. & Davis, N. E. 1957 *Met. Mag.* **86**, 138.

Haurwitz, B. 1941 *Dynamic Meteorology*. New York: McGraw-Hill.

Lettau, H. 1936 *Beitr. Phys. frei. Atmos.* **23**, 45.

Mastenbrook, H. J. & Anderson, A. D. 1953 *Naval Res. Lab. Memo. Rep.* no. 240.

Murray, R. 1954 *Prof. Notes, Met. Off., Lond.*, no. 110.

Richardson, L. F. & Proctor, D. 1925 *Mem. Roy. Met. Soc.* **1**, no. 1.

Solot, S. B. & Darling, E. M. 1958 *Geophys. Res. Papers*, no. 58, Air Force Cambridge Research Center, Bedford, Mass.

Sutton, O. G. 1932 *Proc. Roy. Soc.* A, **135**, 158.
Sutton, O. G. 1953 *Micrometeorology*. New York: McGraw-Hill.
Taylor, G. I. 1921 *Proc. Lond. Math. Soc.* **20**, 196.

Appendix I

Standard vector deviation S of end-points of trajectories after various times

(N = number of trajectories, T = period of initiation)

A. Cases at 300 mb

	July 1947 $N=30$, $T=30$ days		February 1948 $N=28$, $T=28$ days	
Time (h)	[x] (km)	S (km)	[x] (km)	S (km)
6	483	423	258	494
12	805	780	610	800
18	970	1060	940	990
24	1160	1210	1190	1180
30	1340	1420	1490	1410
36	1420	1570	1680	1580
42	1570	1760	1900	1750
48	1730	1820	2100	1890

B. Cases at 500 mb

	Oct. 1949 $N=31$, $T=31$ days		Nov. 1949 $N=30$, $T=30$ days		Dec. 1949 $N=31$, $T=31$ days		Oct.–Dec. 1949 $N=92$, $T=92$ days	
Time (h)	[x] (km)	S (km)	[x] (km)	S (km)	[x] (km)	S (km)	[x] (km)	S (km)
6	197	364	87	302	183	226	150	310
12	442	688	218	509	372	424	330	566
18	690	1042	380	658	541	583	523	800
24	980	1337	510	890	770	744	755	1050
30	1291	1600	682	1100	1066	882	1030	1270
36	1630	1675	897	1378	1375	1028	1330	1430
42	1924	1870	1033	1562	1710	1160	1620	1630
48	2255	1973	1253	1760	2100	1285	1950	1770
54	2485	2087	1500	1915	2358	1427	2225	1910
60	2655	2155	1710	2042	2750	1598	2530	2060
66	2820	2155	1937	2157	2840	1827	2700	2110
72	—	—	2250	2205	3530	2035	2800	2170

C. Cases at 700 mb

	1–15 Aug. 1947 $N=30$, $T=15$ days		1–15 Nov. 1947 $N=30$, $T=15$ days	
Time (h)	[x] (km)	S (km)	[x] (km)	S (km)
6	124	83	211	171
12	237	209	417	362
18	409	266	597	510
24	513	344	765	687
30	666	390	905	805
36	887	430	1100	950
42	1026	460	1288	1098
48	1253	521	1500	1198
54	—	—	1742	1293
60	—	—	1975	1391

D. Cases at 700 mb

	Apr. 1948 $N=15$, $T=30$ days		May 1948 $N=16$, $T=31$ days		June 1948 $N=15$, $T=30$ days		Apr.–June 1948 $N=46$, $T=91$ days	
Time (h)	[x] (km)	S (km)	[x] (km)	S (km)	[x] (km)	S (km)	[x] (km)	S (km)
6	198	225	81	166	25	123	98	192
12	392	462	161	317	51	245	193	363
18	500	603	197	464	103	352	252	482
24	575	727	260	617	129	458	297	650
36	915	922	405	838	167	644	462	888
48	1255	1162	489	985	240	933	621	1142
60	1685	1435	563	1208	312	1168	801	1436
72	2045	1630	710	1357	423	1343	1014	1686

E. Cases at 700 mb

	17 Apr.– 4 May 1950 $N=32$, $T=16$ days		5–20 May 1950 $N=32$, $T=16$ days		1–15 June 1950 $N=30$, $T=15$ days		17 Apr.– 15 June 1950 $N=94$, $T=47$ days	
Time (h)	[x] (km)	S (km)	[x] (km)	S (km)	[x] (km)	S (km)	[x] (km)	S (km)
6	99	181	96	138	81	135	89	155
12	203	339	197	240	176	226	186	274
18	317	470	328	349	262	340	302	393
24	408	604	441	440	358	432	397	501
30	523	754	565	523	447	534	510	618
36	600	947	670	576	533	628	600	743
42	717	1067	805	682	621	747	716	853
48	837	1174	885	756	722	856	815	950
54	972	1325	975	832	810	968	912	1064
60	1127	1415	1110	914	867	1049	1046	1157
66	1244	1520	1225	995	1130	1220	1195	1270
72	1389	1613	1387	965	1410	1358	1388	1348

F. Cases at 700 mb

	1–20 Feb. 1948 $N=40$, $T=20$ days		July 1949 $N=20$, $T=20$ days		Aug. 1949 $N=20$, $T=20$ days	
Time (h)	[x] (km)	S (km)	[x] (km)	S (km)	[x] (km)	S (km)
6	375	261	134	160	171	230
12	675	490	223	317	287	450
18	918	629	329	469	453	631
24	1113	807	405	615	594	827
30	1327	987	480	759	749	973
36	1549	1160	547	887	887	1137

G. Surface cases ($N = 18$, $T = 24$ h)

Time (h)	21–22 Sept. 1943 [x] (km)	21–22 Sept. 1943 S (km)	25–26 Sept. 1943 [x] (km)	25–26 Sept. 1943 S (km)	3–4 Mar. 1944 [x] (km)	3–4 Mar. 1944 S (km)	6–7 Mar. 1944 [x] (km)	6–7 Mar. 1944 S (km)
3	87	54	49	44	105	31	77	21
6	183	103	90	79	202	63	145	43
9	275	144	174	103	295	94	201	59
12	375	186	261	144	407	113	254	71
15	472	223	351	158	502	148	311	88
18	554	257	453	180	613	167	345	113
21	618	293	528	191	709	210	419	134
24	671	331	611	197	792	247	496	150

Time (h)	16–17 June 1944 [x] (km)	16–17 June 1944 S (km)	22–23 June 1944 [x] (km)	22–23 June 1944 S (km)	12–13 Dec. 1944 [x] (km)	12–13 Dec. 1944 S (km)	16–17 Dec. 1944 [x] (km)	16–17 Dec. 1944 S (km)
3	81	75	45	28	77	17	82	26
6	168	138	88	59	151	37	165	59
9	253	194	130	79	225	48	236	81
12	321	242	167	91	300	55	300	104
15	381	283	201	89	378	61	378	143
18	447	321	244	79	452	68	453	169
21	504	365	290	81	520	80	527	195
24	553	365	343	95	587	93	585	225

Appendix II

The values of σ over Southern England

The standard deviation of wind $\sigma(T)$ taken over periods of duration T bears a ratio to the standard deviation σ' over a long period depending on the value of T.

Some ratios have been set out in tables A and B. Table A was derived from the comparison of winds at 500 mb observed during 15 years at Larkhill (or Crawley) in the months of January and July. Table B was derived from data given by Durst (1954) which enabled the ratio of $\sigma(T)$ to σ' to be calculated.

T	1 day	2 days	4 days	8 days	1 mth.	3 mth.	5 mth.	15 mth.
January $\sigma(T)$	17·7	24·4	29·4	32·6	38·8	40·6	41·6	41·8
$\sigma(T)/\sigma$ (15 mth.)	0·40	0·58	0·70	0·78	0·93	0·97	0·99	1·00
July $\sigma(T)$	11·6	16·2	19·4	22·6	28·4	29·3	29·5	29·6
$\sigma(T)/\sigma$ (15 mth.)	0·39	0·55	0·65	0·76	0·96	0·99	1·00	1·00

TABLE A. Value of $\sigma(T)$ in knots for various values of T

T	5 min.	15 min.	30 min.	1 h	6 h	12 h	24 h
$\sigma(T)/\sigma'$	0·037	0·062	0·088	0·111	0·22	0·30	0·41

TABLE B. Values of $\sigma(T)/\sigma'$ for various values of T

σ' is the long period value of the standard vector deviation of wind, which is a constant for the appropriate region, season and level.